Single-electron transistor made of multiwalled carbon nanotube using scanning probe manipulation

Leif Roschier,[a] Jari Penttilä, Michel Martin, Pertti Hakonen, and Mikko Paalanen
Low Temperature Laboratory, Helsinki University of Technology, FIN-02015 HUT, Finland

Unto Tapper and Esko I. Kauppinen
VTT Chemical Technology, VTT Aerosol Technology Group, FIN-02044 VTT, Finland

Catherine Journet and Patrick Bernier
Universite Montpellier II, 34095 Montpellier Cedex 05, France

(Received 15 April 1999; accepted for publication 7 June 1999)

We positioned semiconducting multiwalled carbon nanotube, using an atomic force microscope, between two gold electrodes at SiO_2 surface. Transport measurements exhibit single-electron effects with a charging energy of 24 K. Using the Coulomb staircase model, the capacitances and resistances between the tube and the electrodes can be characterized in detail. © *1999 American Institute of Physics.* [S0003-6951(99)00131-X]

Carbon nanotubes[1] represent a new building block for nanotechnology and nanoelectronics. They may be considered as graphite sheets wrapped into seamless cylinders. The two types of nanotubes are multiwalled carbon nanotube (MWNT), where many tubes are arranged in a coaxial fashion, and a single-walled nanotube (SWNT), consisting of only a single layer. The tubes are either metallic, semimetallic or semiconducting depending on how the graphite sheets are wrapped around.[2] The electrical properties of the carbon nanotubes have been exploited, e.g., in single-electron transistor (SET) made of ropes of SWNTs[3] and in a room temperature transistor made of SWNT.[4] There are also investigations on the resistance of a nanotube/metal-contact system,[5] and on soldering a low-ohmic contact using an electron beam.[6]

Since the early work by Junno *et al.*,[7] scanning probe microscopes (SPM) have been utilized for manipulation of small metal particles.[8,9] Also MWNTs have been moved using SPM[10] and they have been a subject in tribological studies of sliding and rolling friction between the nanotube and the substrate.[11] In this letter, we report a MWNT single electronics device fabricated using scanning probe manipulation. This may be considered as a new fabrication method towards molecular electronics.

The MWNTs used in our experiment were prepared by arc-discharge method with 100 A current and 30 V voltage at 660 mbar helium atmosphere. They were purified for 45 min in ambient air at 750 °C temperature. Afterwards the tubes were dispersed in isopropanol and mixed ultrasonically. A drop of this solution was deposited on the substrate, which was then kept in isopropanol atmosphere for 5 min. Then the droplet was blown off with dry nitrogen gas. Figure 1 illustrates transmission electron microscope (TEM) images of tubes taken from the same solution as the measured one. There is some surface roughness which may affect the tunneling resistance between the tube and the electrode.

The electrode structure was fabricated using electron-beam lithography on a $6\times10\ mm^2$ substrate cut from an oxidized silicon wafer. The 60 nm wide electrodes consist of a 2 nm thick layer of chromium (for adhesion) and a 14 nm thick layer of gold. The distance between the electrodes was 250 nm and the distance between a side gate and the electrodes was around 500 nm. The substrate was cleaned in oxygen plasma before the deposition of the tube.

We used Park Scientific Instruments (PSI) CP AFM with Ultralever cantilevers to image the surface and to move one of the MWNTs on top of it. We operated the atomic force microscope (AFM) in noncontact mode (NCM) as it was used, e.g., to move silver aerosol particles over SiO_2 surface.[8] The ProScan software from PSI was used to control the AFM. The moved MWNT was about 410 nm long and its diameter was 20 nm. The tube was moved with the following procedure. First, the surface was imaged in a standard way in NCM with the feedback loop on. Then, the tip was positioned to scan along a single line over the tube end. The feedback loop was cut off and the tip surface distance was decreased in small steps (1–10 nm). Simultaneously, the vibration amplitude (NCM amplitude in the software) was

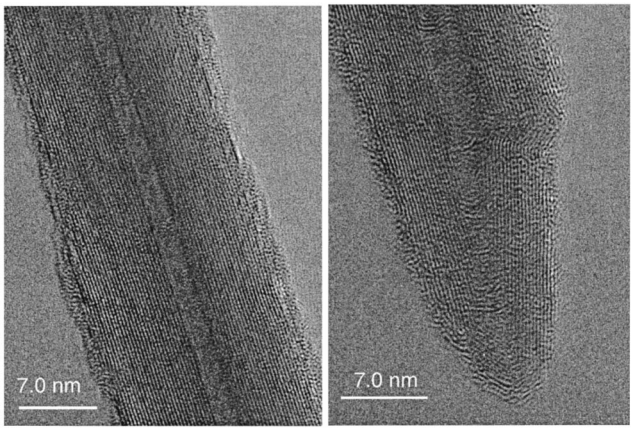

FIG. 1. Transmission electron microscope images of our MWNTs. The shape and roughness corresponds to those reported by other groups (see Ref. 12).

[a]Electronic mail: leif.roschier@hut.fi

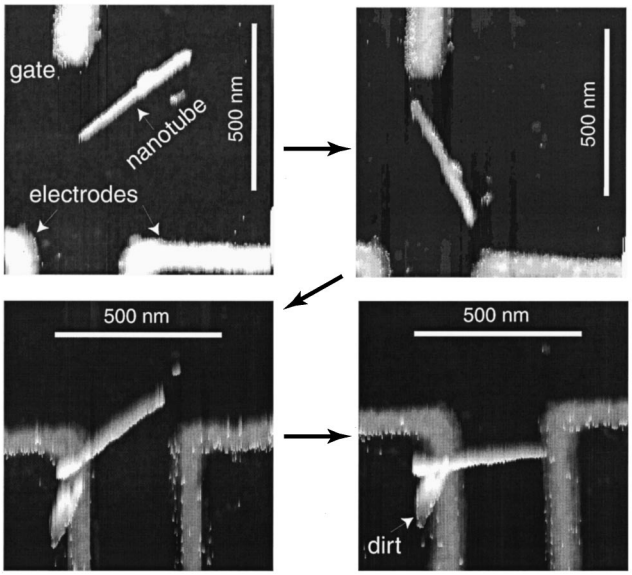

FIG. 2. AFM images during moving process. The 410 nm long MWNT, the side gate and the electrode structure are marked in the first frame. The last frame represents the measured configuration, where one end of the MWNT is well over the left electrode and the other end is lightly touching the right electrode.

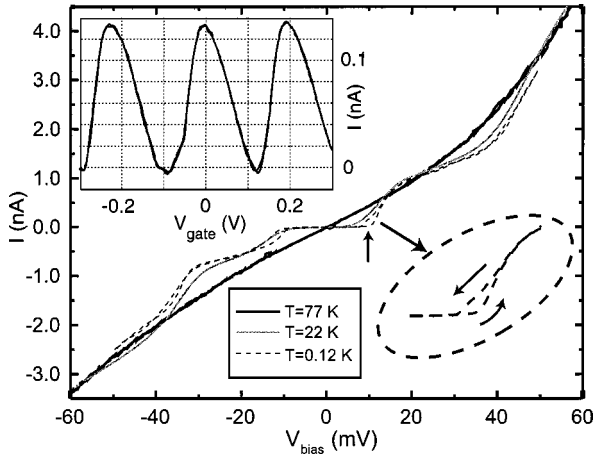

FIG. 3. Measured $I(V_{\text{bias}})$ curves at different temperatures when the gate is at zero-bias. The inset shows the gate modulation at $V_{\text{bias}}=10$ mV (indicated by the arrow) at $T=120$ mK. The enlargement in down-right corner shows the hysteretic behavior of the current in more detail.

monitored. As the distance was decreased, the vibration amplitude decreased and the tube location along the scanline could be observed *in situ*. At the stage when the tube was hardly anymore visible in the amplitude signal, the tube usually moved. The first step to get the tube loose differed from all the other ones so that the tip had to be pushed much harder against the surface. The tube moved as rotations around a pivot point like in Ref. 11. In $\frac{1}{3}$ of the cases, the rotation took place in the opposite direction than was intended. In these cases, the AFM tip dragged the tube. The intended moving procedure was to push the tube end, which happened in the remaining $\frac{2}{3}$ of the cases. Thus, the moving procedure was a trial and error iterative process and lasted a couple of days (≈ 100 pushes/images). The distance between the original and final position of the tube was over 1 μm. Figure 2 displays a selection of AFM images taken in the course of the moving process. Note that it was possible to lift the nanotube on top of the electrode which has a thickness larger than the tube radius.

The electric measurements of the tube/electrode system were done at low temperatures with a plastic dilution refrigerator. The sample resistance, tracked using 100 mV dc voltage, increased from 5 to 9 MΩ, when cooling from 300 K down to 4 K. Most of this resistance is due to the Au/C contacts (tunnel junctions) which are known to be rather resistive.[5] As for the conduction along the multiwalled nanotube, we expect our experiments to probe the outermost shell. This is because the section over which we are measuring the conductance is only 300 nm long, i.e., about 1000 atomic spacings. Over such a short distance the intralayer conductance can be neglected, since it is expected to be 10^{-5} times smaller than the in-plane value as in graphite.[13] Owing to the small conductance of the sample, constant voltage biasing with one end grounded was employed in our measurements.

The measured $I-V$ curves display a 15 mV wide zero current plateau across zero-voltage bias as illustrated in Fig. 3. The plateau is visible at 22 K temperature but not anymore at 77 K. The shape of $I(V_{\text{bias}})$ curve is mostly due to the density of states with a gap and it shows that electron and hole transports are fairly equal. Coulomb effects become clearly observable below a few Kelvin and the nanotube behaves as a SET. The asymmetry of the gate modulation, illustrated in the inset for $V_{\text{bias}}=10$ mV, indicates a substantial difference in the resistances of the tunnel junctions; even larger asymmetry in $I(V_{\text{gate}})$ was recorded at smaller V_{bias}. The modulation period yields $C_g=0.8$ aF for the gate capacitance of the SET. There is clear hysteresis in the $I(V_{\text{bias}})$ curves at $T=120$ mK in Fig. 3. We believe this phenomenon can be attributed to charge trapping,[14] in which single electrons tunnel hysteretically across the concentric tubes.

Figure 4 illustrates surface and contour plots constructed from $I(V_{\text{gate}})$ curves at different V_{bias} values at $T=120$ mK. The gate modulation is visible, but it cannot make the tube to conduct at zero bias voltage. This is a signature of a semiconducting nanotube. The single set of parallel ridges in the $I(V_{\text{gate}},V_{\text{bias}})$ surface matches the Coulomb staircase model, where the resistances of tunnel junctions differ appreciably.[15] Hence, the current through the MWNT is determined mostly by the junction with larger tunnel resistance. In this case, the ridges are remnants of the Coulomb steps that are fully visible in a single electron box. The physical requirements imposed by such a Coulomb staircase model on the tunnel resistances agree with our AFM images which indicate that, owing to the larger overlap area, the left tunnel junction is much more conducting than the right one (see the last frame of Fig. 2).

Assuming that, as in the case of superconductors, the gaps due to the density of states and due to Coulomb blockade both affect $I-V$ characteristic, we can relate slopes of the constant current curves (the minima and maxima of $(\partial V_{\text{bias}}/\partial V_{\text{gate}})|_{I=\text{const}}$) at the conduction threshold with the ratios C_g/C_{right} and C_g/C_{left}. Using the slopes marked in Fig. 4(b), we obtain $C_{\text{left}}=26$ aF and $C_{\text{right}}=11$ aF for the capacitances between the tube and the left/right electrode, respectively. In fact, in the determination of the latter value, we gave more weight to the slope of the ridges than for the

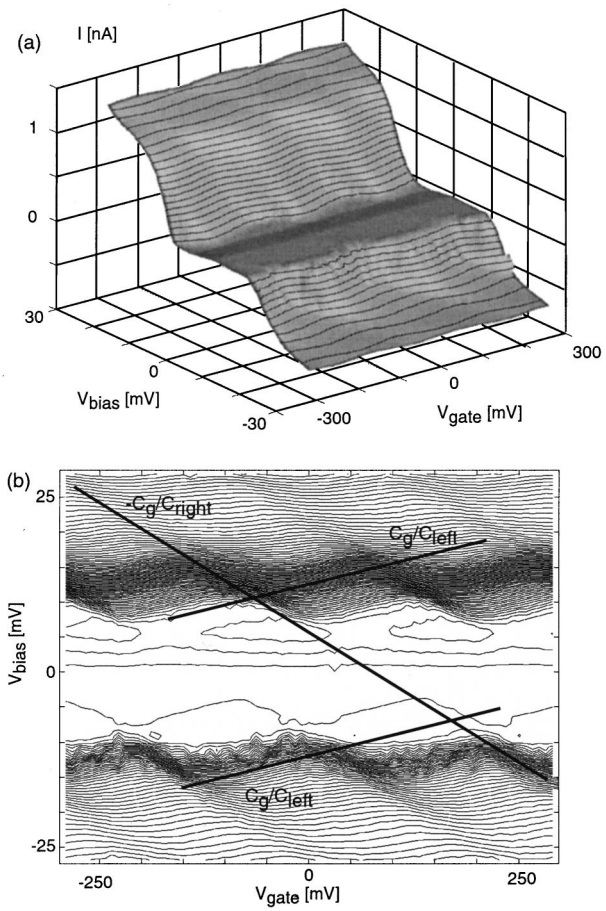

FIG. 4. (a) $I(V_{\text{bias}}, V_{\text{gate}})$-surface constructed from $I(V_{\text{gate}})$ data at different V_{bias} values. (b) The same data represented as a constant-current contour plot illustrating more clearly the ridges due to the Coulomb staircase.

conduction edge: the positions of the ridges are less sensitive to the density of states than the slopes of the sawtooth pattern. As expected, the larger value corresponds to the junction with larger overlap area between the electrode and the nanotube. The total capacitance yields for the charging energy $E_c = e^2/2(C_{\text{left}} + C_{\text{right}} + C_g) = 2.1\,\text{meV}$.

We want to emphasize that all our values rely on data measured above the semiconducting gap where the density of states is dependent on the voltage in a nontrivial fashion. Therefore, those values that are based on the assumption of metallic, constant density of states must be viewed with consideration. The resistance of the better conducting tunnel junction is not an easy-to-define quantity at the conduction edge: its value from the gate modulation curve asymmetry falls into the range $R_{\text{left}} = 0.5\text{–}1.5\,\text{M}\Omega$. For the less conducting junction, we obtain $R_{\text{right}} = 8\,\text{M}\Omega$. Unfortunately, it is impossible to estimate resistances reliably from the overlap area measured in the AFM images since most of the electron tunneling may happen in a small protrusion of the tube due to the exponential nature of the tunneling process.

In summary, we have manufactured a MWNT-based SET using AFM manipulation and measured its current–voltage characteristics. We saw single-electron charging effects via gate modulation. The results imply the MWNT to be semiconducting with a gap of 15 meV. The Coulomb staircase structure in the data agrees with the asymmetry of the tunnel junctions. Our method combined with electron-beam ''soldering'' may open new possibilities to optimize junction parameters for specific purposes. This could give new opportunities in the fabrication of single electron transistors.

The authors want to thank M. Ahlskog, P. Arseev, C. Schönenberger and E. Sonin for useful discussions. This work was supported by the Academy of Finland, by TEKES of Finland via the Nanotechnology program, and by the Human Capital and Mobility Program ULTI of the European Community.

[1] S. Iijima, Nature (London) **354**, 56 (1991).
[2] J. W. Mintmire, B. I. Dunlap, and C. T. White, Phys. Rev. Lett. **86**, 631 (1992); N. Hamada, S. Sawada, and A. Oshiyama, *ibid.* **86**, 1579 (1992); R. Saito, M. Fujima, G. Dresselhaus, and M. S. Dresselhaus, Appl. Phys. Lett. **60**, 2204 (1992).
[3] M. Bockrath, D. H. Cobden, P. L. McEuen, N. G. Chopra, A. Zettl, A. Thess, and R. E. Smalley, Science **275**, 1922 (1997).
[4] S. J. Tans, M. H. Devoret, H. Dai, A. Thess, R. S. Smalley, L. J. Geerlings, and C. Dekker, Nature (London) **386**, 474 (1997); S. J. Tans, A. R. M. Verschueren, and C. Dekker, *ibid.* **393**, 49 (1998).
[5] P. J. de Pablo, E. Graugnard, B. Walsh, R. P. Andres, S. Datta, and R. Reifenberger, Appl. Phys. Lett. **74**, 323 (1999).
[6] A. Bachtold, M. Henny, C. Terrier, C. Strunk, C. Schönenberger, J.-P. Salvetat, J.-M. Bonard, and L. Forrò, Appl. Phys. Lett. **73**, 274 (1998).
[7] T. Junno, K. Deppert, L. Montelius, and L. Samuelson, Appl. Phys. Lett. **66**, 3627 (1995).
[8] M. Martin, L. Roschier, P. Hakonen, Ü. Parts, M. Paalanen, B. Schleicher, and E. I. Kauppinen, Appl. Phys. Lett. **73**, 1505 (1998).
[9] T. R. Ramachandran, C. Bauer, A. Bugacov, A. Madhukar, B. E. Koel, A. Requicha, and C. Gazen, Nanotechnology **9**, 237 (1998).
[10] T. Hertel, R. Martel, and P. Avouris, J. Phys. Chem. B **102**, 910 (1998).
[11] M. R. Falvo, R. M. Taylor, A. Helser, V. Chi, F. P. Brooks, Jr., S. Washburn, and R. Superfine, Nature (London) **397**, 236 (1999).
[12] *Handbook of Microscopy, Applications in Materials Science, Solid-State Physics and Chemistry*, edited by S. Amelinckx, D. van Dyck, J. van Landuyt, and G. van Tendeloo (VCH, Weinheim, 1997), p. 458.
[13] B. T. Kelly, *Physics of Graphite* (Applied Science, London, 1981), p. 294.
[14] P. D. Dresselhaus, L. Ji, Siyuan Han, J. E. Lukens, and K. K. Likharev, Phys. Rev. Lett. **72**, 3226 (1994).
[15] See, e.g., A. E. Hanna and M. Tinkham, Phys. Rev. B **44**, 5919 (1991).